

## Design and characterization of 225–370 GHz DSB and 250–360 GHz SSB full height waveguide SIS mixers

*A.Navarrini, B.Lazareff, D.Billon-Pierron, and I.Peron*

*IRAM (Institut de Radio Astronomie Millimétrique)*

*300, rue de la Piscine – 38406 St. Martin d'Hères Cedex – France*

### **Abstract**

We describe the design, construction, and characterization of two SIS mixers: a DSB mixer for the band 275–370 GHz, intended for band 7 of the ALMA frontend, and a SSB mixer, backshort tuned, intended for IRAM's Plateau de Bure interferometer, and covering the band 260–360 GHz. These two mixers share various common design features, such as a wideband single ended probe transition from full height waveguide to microstrip, and they use the same mixer chip. A significant challenge, especially for the SSB mixer, has been to achieve not only low noise, but also stable operation over the design band. The receiver noise for the DSB mixer is found to be below 50 K over 100 GHz of RF bandwidth, with a minimum as low as 27 K (uncorrected) at 336 GHz. The SSB receiver has a measured image rejection of order –14dB over the design band, and its noise remains below 80 K (effectively a SSB receiver noise value).

### **1 Introduction**

The frontend for the ALMA project comprises ten frequency bands, among which band 7 (275–370 GHz), whose baseline specification is for a DSB, fixed-tuned mixer, with a maximum noise temperature of  $5h\nu/k$  (66 K at 275 GHz). Therefore, our first goal has been to develop a low-noise DSB mixer with stable operation over that band.

A significant element of the system noise in a mm-wave frontend is the atmosphere's radiation in the image band. The new receivers being developed for IRAM's Plateau de Bure interferometer include a channel covering the band 260–360 GHz; it is foreseen to reject the image band with an adjustable backshort, as in current IRAM receivers. Therefore, the second goal of our work has been to develop such an SSB mixer, again with low noise and stable operation.

### **2 Design**

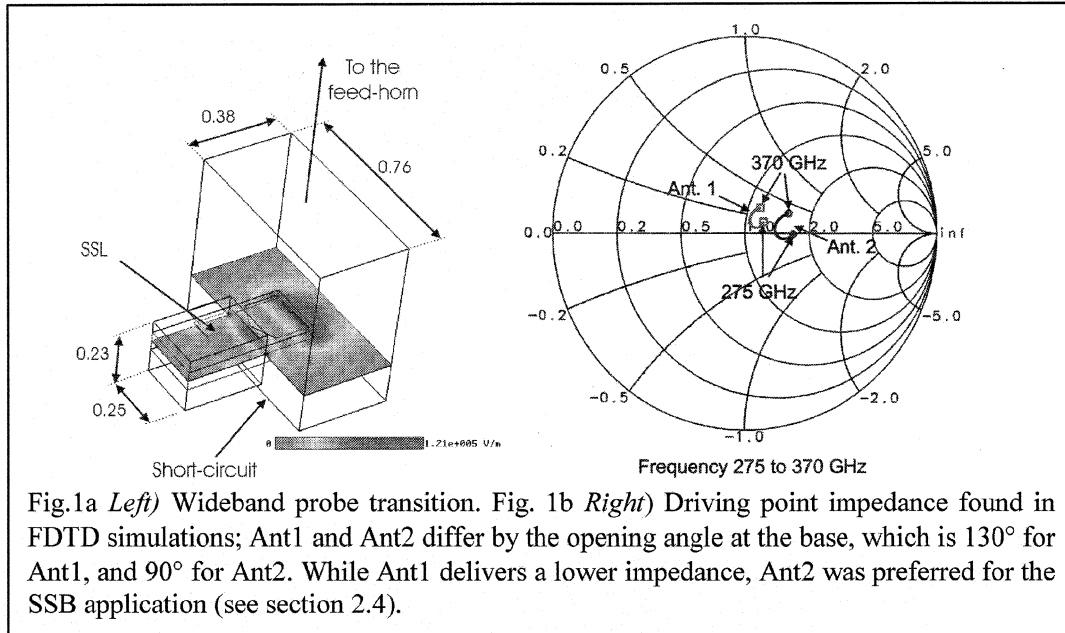
In the section we review the main design features of the two mixers, referring the reader to Navarrini *et al* [1], where the design of the SSB mixer is presented in more detail.

#### **2.1 Full height waveguide to microstrip transition**

One of the goals of the design is to achieve an efficient coupling of the available RF energy to the SIS junction. Rather than attempting a global optimization, we have, as a first step, optimized the coupling of the waveguide  $TE_{10}$  mode to a TEM port with real and suitably low impedance. We chose to use full height waveguide for these mixers, because, compared with reduced height waveguide, it has lower losses and is easier to fabricate.

##### **2.1.1 Wideband probe transition**

Yassin and Withington [2] have shown that a very good match can be obtained between a full-height waveguide and the driving point impedance of a radial probe, with a real



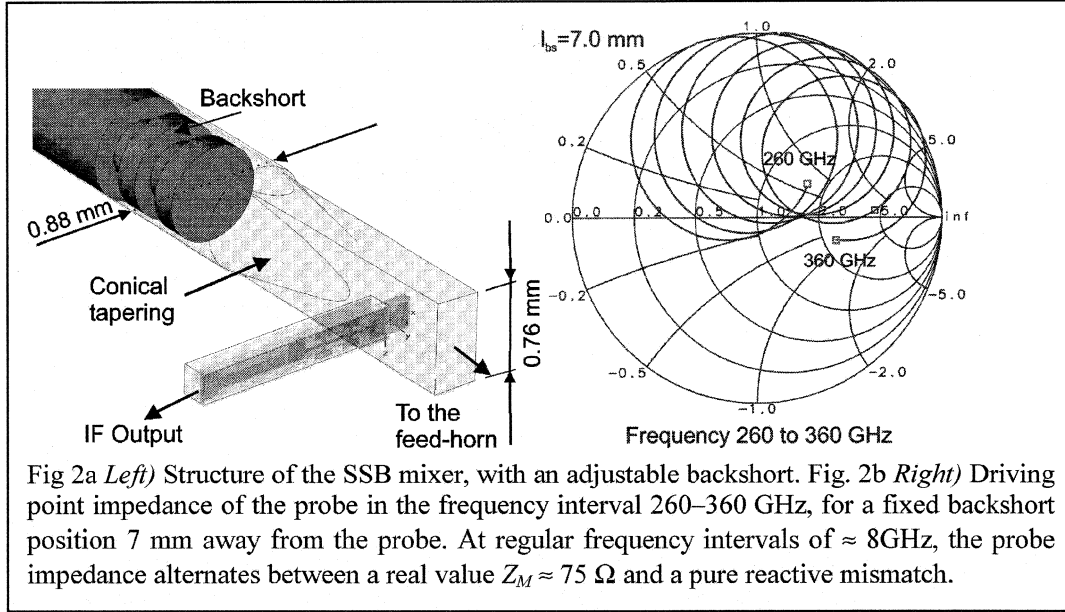
and relatively low value ( $\approx 50 \Omega$ ) over a full waveguide band. In a practical implementation, the antenna drives a microstrip line whose ground plane is a suspended stripline RF choke sitting on a dielectric substrate, itself housed in a channel perpendicular to the waveguide (see Fig. 1a).

We modeled this configuration using the FDTD package Microwave Studio from CST [3]. We obtained for the driving point impedance the results shown on Fig. 1b, with the following parameters: waveguide dimensions  $760 \mu\text{m} \times 380 \mu\text{m}$ , substrate fused quartz, width  $250 \mu\text{m}$ , thickness  $80 \mu\text{m}$ ,  $100 \mu\text{m}$  air above,  $50 \mu\text{m}$  air below, probe (and substrate) extending  $200 \mu\text{m}$  into the waveguide, opening angle at probe base  $90^\circ$ . The fixed backshort is located at  $210 \mu\text{m}$  behind the plane of the probe metallization, approximately  $\frac{1}{4} \lambda_g$ . An impedance close to  $75 \Omega$  is obtained over the band 275-370 GHz. While Yassin and Withington show that good results can be obtained with the probe either in the longitudinal plane or perpendicular to the waveguide, we chose the latter orientation in order to decouple the  $\text{TE}_{10}$  mode of the waveguide from an odd-symmetry mode of the suspended stripline, whose cutoff frequency falls within the operating band.

### 2.1.2 Image rejection by reactive termination.

If the electrical distance between the probe and the backshort is an integer multiple of  $\frac{1}{2} \lambda_g$ , the probe is shorted, and the junction sees a reactive termination; if that distance is an odd multiple of  $\frac{1}{4} \lambda_g$ , a match is obtained for the probe, and for the junction, provided that a proper matching circuit is present (will be discussed further down). For given values of the signal and image frequencies,  $\nu_s$  and  $\nu_i$ , the two conditions can be met (approximately) for the same backshort position  $l_{bs}$  (see [1]):

$$l_{bs} = \frac{c}{8\nu_{IF}} \sqrt{1 - \left( \frac{\nu_c}{\nu_{LO}} \right)^2} \quad (1)$$



For an IF center frequency of 4 GHz,  $l_{bs} \approx 7$  mm. Figure 2 shows the structure of the SSB mixer, and the modeled probe impedance as function of frequency for an arbitrary backshort position. Equation (1) only gives an approximate value for  $l_{bs}$ , the precise value is chosen to have maximum rejection at  $\nu_I$  (and a near optimum match at  $\nu_S$ ).

## 2.2 Stability

### 2.2.1 DSB case

In the DSB case, the LSB and USB ports of the junction see equal terminations (actually, in the formalism of Tucker's theory, because  $\nu_L \equiv \nu_I = \nu_{IF} - \nu_{LO}$  is negative,  $Y_{-I} = Y_I^*$ ). The output impedance at the junction's IF port, defined by (using standard notations):

$$Y_{IF} = Z_{00}^{-1} - Y_0 \quad (2)$$

is actually independent of  $Y_0$ . If the mixer is to be stable for arbitrary passive IF load admittance  $Y_0$ , the real part of  $Y_{IF}$  must be positive. Fixing the bias voltage at the middle of the photon step:  $V_{DC} = V_g - h\nu_{LO}/2e$ , and the pumping parameter  $\alpha = 1$ , leaves as the only free parameter the RF impedance  $Y_I$  seen by the junction. The region of stability, that depends only weakly on the LO frequency, is shown on Fig. 3a. This problem had already been discussed by D'Addario [4].

### 2.2.2 SSB case

In the SSB case, to keep the discussion manageable, we *assume* that the junction sees on the signal port a source impedance  $Z_S = R_N$ . As discussed above, the rejection of the image frequency is achieved by presenting a pure reactive termination  $Z_I$  on that port, whose value is the only free parameter in this case. The stability condition (again weakly dependent on frequency) is more restrictive at the low end of the operating range; at 275 GHz, the stable region is given by:

$$-3.27 \leq \frac{Z_I}{jR_N} \leq +0.12 \quad (3)$$

This portion of the  $\Gamma = 1$  circle is shown on Fig.3b.

### 2.3 Junction parameters

To achieve the RF tuning bandwidth of  $\approx 100$  GHz, we chose a  $R_N \times A$  product of  $25\Omega \times \mu\text{m}^2$ . With a specific capacitance of  $75 \text{ fF} \times \mu\text{m}^{-2}$ , this corresponds to a quality factor  $Q = R_{RF}C\omega = 2.6$  at mid-band, based on a small-signal RF impedance  $R_{RF} = 0.75 \times R_N$  at 310 GHz. A junction area of  $1 \mu\text{m}^2$  was chosen as a compromise between the technological difficulties of fabricating small area junctions with a good accuracy, and the problem of matching the junction's RF impedance to the higher driving point impedance of the waveguide probe. The junction definition was realized by E-beam lithography.

### 2.4 Matching circuit

The matching circuit is realized by a combination of microstrip lines patterned in the Nb wiring layer over a 200 nm  $\text{SiO}_2$  ( $\epsilon=4.2$ ) insulation, and sections of coplanar waveguide patterned in the base Nb of the trilayer. The junction capacitance is tuned out by a short ( $\approx \lambda/8$ ) length of microstrip line terminated to a virtual ground provided by a radial stub. The resulting near-real impedance is matched to the waveguide probe by a  $\lambda/4$  transformer, realized as a capacitively loaded coplanar waveguide, comprising two coplanar sections. The probe with a  $90^\circ$  opening angle was chosen (see Fig.1) despite the higher transformation ratio to  $75 \Omega$ , because it allows to better fulfill the stability criterion for the SSB mixer.

The design was performed by computing the S-parameters of the probe coupling structure (including the suspended substrate microstrip line choke) with CST Microwave Studio [1], and of the planar circuit discontinuities with Sonnet [5], and then importing these into ADS [6] where the optimization of microstrip and coplanar transmission line lengths was performed. As can be seen on Fig. 3, this circuit provides

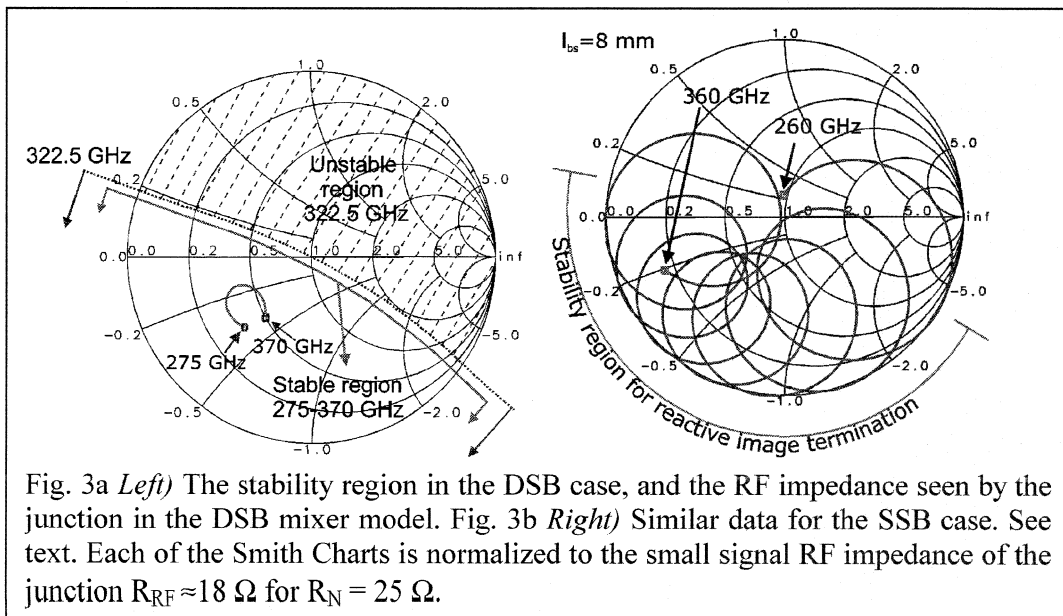
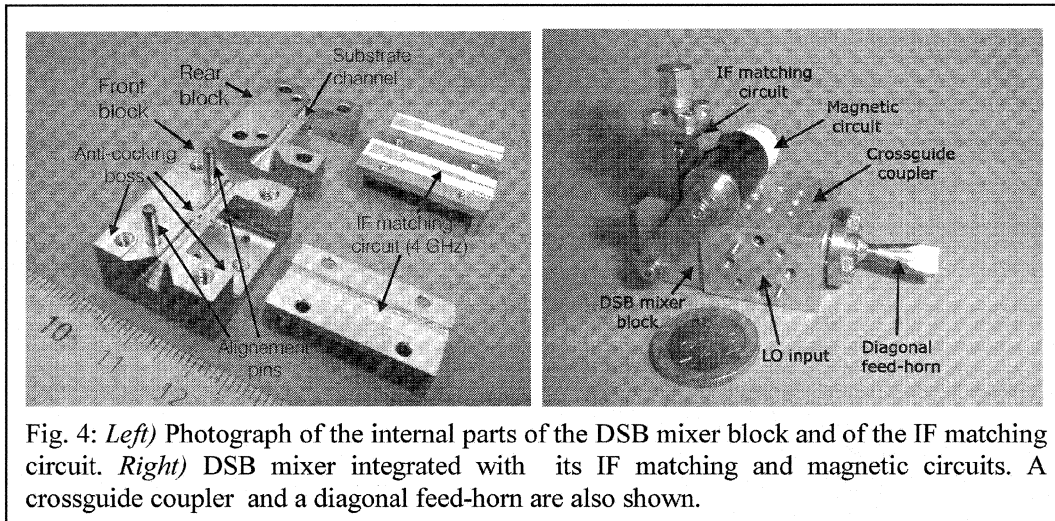


Fig. 3a *Left*) The stability region in the DSB case, and the RF impedance seen by the junction in the DSB mixer model. Fig. 3b *Right*) Similar data for the SSB case. See text. Each of the Smith Charts is normalized to the small signal RF impedance of the junction  $R_{RF} \approx 18 \Omega$  for  $R_N = 25 \Omega$ .

a broadband match for the DSB mixer, a good match at the signal frequency for the SSB mixer, and fulfils the respective stability criteria for either type of mixer.

### 3 Experimental results

The main parts of both DSB and SSB mixer blocks are made of brass and are split in two parts (Fig. 4). The front block is identical in the two mixers and includes the full height waveguide realized by spark erosion. Anti-cocking bosses and alignment pins are used the front blocks. Both mixers include magnetic circuits for the suppression of the Josephson current.



The receiver noise was obtained by the standard method placing ambient temperature and cold (77 K) loads in front of the receiver. We assumed the effective temperature of the radiating loads to equal the physical temperature (Rayleigh-Jeans approximation). This also corresponds with very good approximation to the Callen&Welton effective radiating temperature [7] that excludes quantum vacuum fluctuation from the receiver noise.

The mixer under test is installed in a two stage liquid helium/liquid nitrogen cryostat for laboratory noise measurements. A 1.78 mm thick grooved HDPE vacuum window and a IR filter realized with a 8.15 mm polystyrene foam are located on the signal path before a corrugated feed-horn with HDPE grooved phase correcting lens. A 3.5-4.5 GHz IF HEMT amplifier with noise  $T_{IF} \approx 5$  K and gain  $G_{IF} \approx 34$  dB is cascaded with the mixer. A Gunn oscillator followed by a frequency multiplier (3 $\times$  or 4 $\times$ ) provides the necessary local oscillator (LO) power over the test band. The mixers have been tested by using LO injection both with *a*) a wire grid located outside the cryostat *b*) a -16 dB branch-guide coupler.

#### 3.1 Characterization of the DSB mixer

The pumped current-voltage characteristic with LO frequency  $\nu_{LO} = 320$  GHz, as well as the receiver output power as a function of bias in response to hot/cold loads are shown in Fig. 5. The receiver noise measured in front of the injection grid at this particular

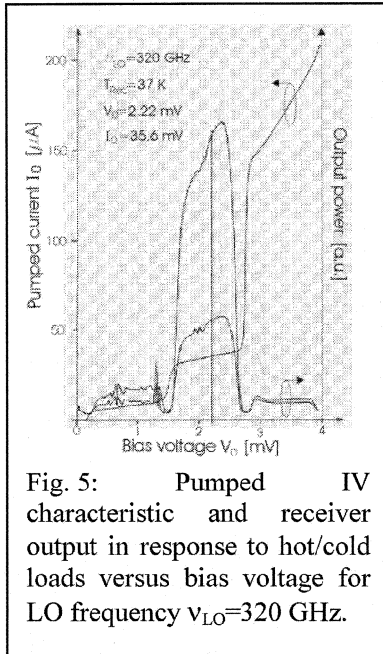


Fig. 5: Pumped IV characteristic and receiver output in response to hot/cold loads versus bias voltage for LO frequency  $v_{LO}=320$  GHz.

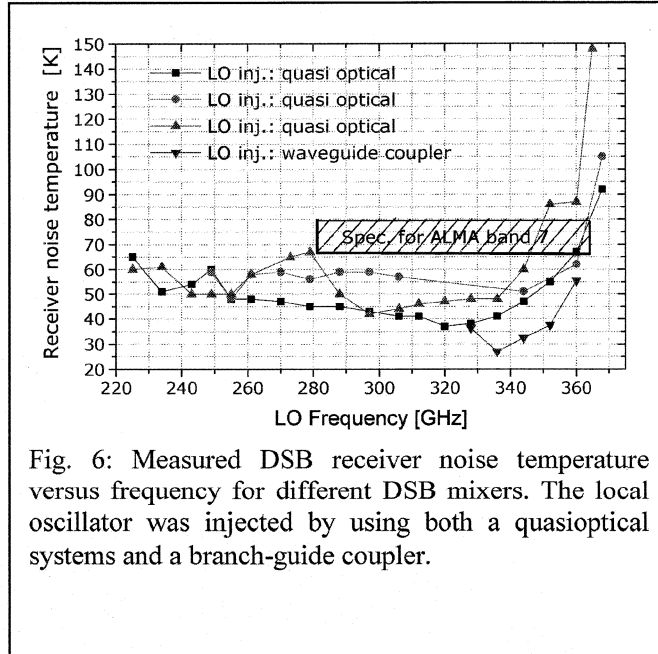


Fig. 6: Measured DSB receiver noise temperature versus frequency for different DSB mixers. The local oscillator was injected by using both a quasi-optical systems and a branch-guide coupler.

frequency was 37 K. Fig. 6 shows the measured receiver noise temperature plotted against LO frequency for various chip-DSB block combination over the 225-368 GHz band. The  $T_{rec}$  measurement are uncorrected for optics and injection losses. The first three measurements were obtained with quasi-optical injection: the receiver noise is below 60 K over more than 100 GHz of band. The relative bandwidth of the mixer of approximately 50 % is one of the widest ever reported. The increase of noise in the upper part of the band is believed to be caused by the junction area being 35 % larger than specified. Even with that increase the specification for the RF coverage of ALMA band 7 is met.

A further test of the mixer using a branch-guide coupler [8] gave superior performance in terms of noise temperature over a narrower bandwidth, with minimum of (uncorrected)  $T_{rec}=27$  K at 336 GHz; to our knowledge this is the lowest receiver noise ever reported at this frequency.

### 3.2 Characterization of the SSB mixer

Setting the mixer for SSB operation at the signal frequency  $v_s$  is a two-step process. First, the LO is set at the image frequency  $v_i$ , and the junction dc pumped current is plotted versus backshort position  $l_{bs}$ . A position that gives minimum current corresponds to minimum coupling of the junction at  $v_i$ . Actually, several positions are found, spaced at regular intervals of  $\lambda_g/2$ , as shown on the experimental result plotted in Fig. 7. Mixer modelling calculations are used to select the position  $l_{bs}$  that gives near-optimum coupling at the signal frequency. Then the LO is set at the proper  $v_{LO}$  for SSB operation at  $v_s$  without changing  $l_{bs}$ . The narrow resonances observed in the plot of

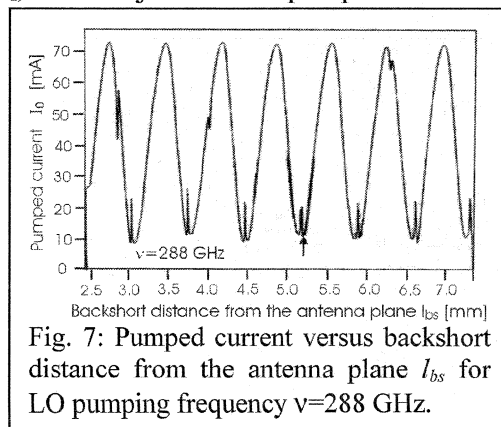
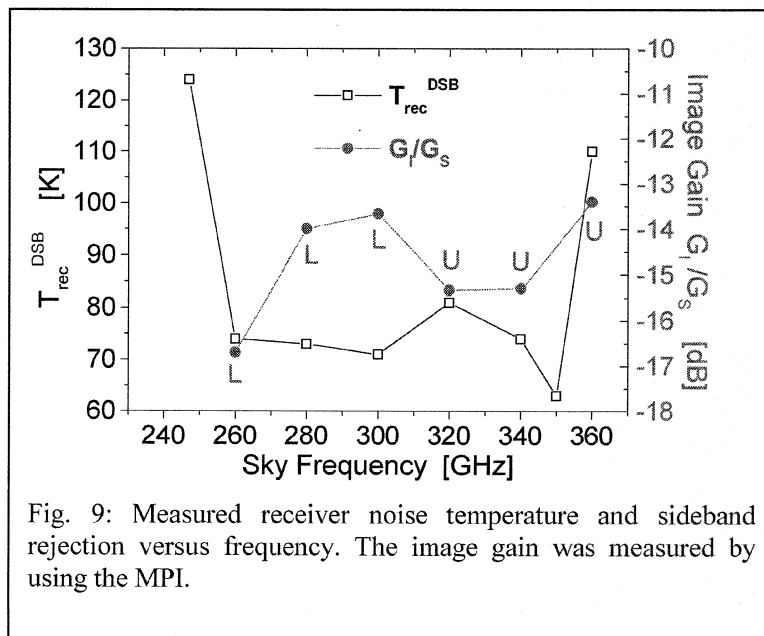
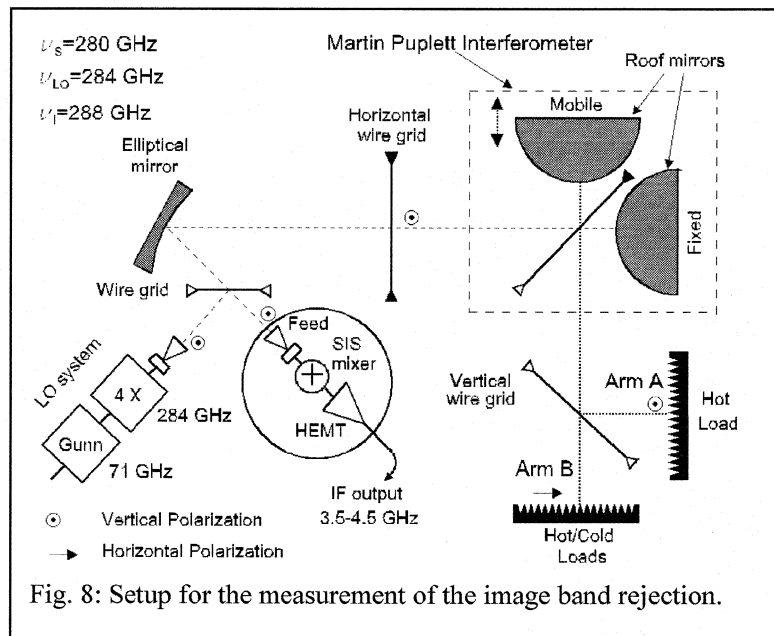


Fig. 7: Pumped current versus backshort distance from the antenna plane  $l_{bs}$  for LO pumping frequency  $v=288$  GHz.

the pumped current versus  $I_{bs}$  curve are believed to be caused by the second polarization of the  $TE_{11}$  mode that can propagate in the circular waveguide. We believe that the second  $TE_{11}$  mode is coupled by an off-axis displacement of the circular backshort and is trapped between the backshort and the transition. The narrow resonances can degrade the image rejection at particular frequencies. Therefore, it is foreseen to replace the circular cross-section backshort with a new choke type rectangular backshort that can be moved in an uniform rectangular waveguide.

The image band rejection has been measured by using a Martin-Puplett Interferometer (MPI) that provides sideband filtering (Fig. 8). The MPI is tuned to reject successively the signal and image band. Then, the difference of the receiver output powers in



response to hot/cold loads located in the arm B are measured. The sideband rejection is obtained as the ratio of these differences.

The results of characterization of the SSB mixer are shown in Fig. 9. A DSB receiver noise temperature of the order of 80 K (uncorrected) is obtained over most part of the band (left scale) with an image rejection around  $-14$  dB (right scale). Given the high image rejection, the plotted receiver noise is an SSB receiver noise temperature apart from a factor  $(1+G_I/G_S)\approx 1.04$ .

#### **4 Conclusions**

Two SIS mixers in full height waveguide have been designed. They use the same mixer chip. One is a fixed tuned DSB mixer, designed for ALMA band 7 (275-370 GHz). Its operation has been demonstrated over 225–370 GHz, with a DSB noise temperature below 50 K over a 100 GHz RF band, the minimum being 27 K at 336 GHz. The second one is a SSB mixer designed for IRAM's Plateau de Bure interferometer, with an RF band 260–360 GHz, and where the rejection of the image band and the matching of the signal band are simultaneously achieved by an adjustable backshort. The measured rejection is of order  $-14$ dB; the (quasi-SSB) receiver noise is below 80 K over 90% of the design band.

#### **References**

- [1] A. Navarrini, D. Billon-Pierron, K.F. Schuster, and B. Lazareff, "Design of a 275-370 GHz SIS mixer with sideband rejection and stable operation", 12<sup>th</sup> International Symposium on Space Terahertz Technology (2001).
- [2] G. Yassin and S. Withington, "Analytical expression for the input impedance of a microstrip probe in waveguide", *Int. J. Infrared and Millimetre Waves*, **17**, 1685-1705, 1996.
- [3] CST, Darmstadt, Germany. <http://www.cst.de>
- [4] L.R. D'Addario. "Noise parameters of SIS mixers" *IEEE Trans. Microwave Theor. Tech.*, **36**, 1196-1206, 1988
- [5] Sonnet Software, <http://www.sonnetsoftware.com>
- [6] ADS, Agilent Technologies, <http://eesof.tm.agilent.com/products/adsoview.html>
- [7] A.R.Kerr, "Suggestions for revised definitions of noise quantities, including quantum effects", *IEEE Trans. Microwave Theor. Tech.*, **47**, 325-329, 1999
- [8] S. Claude, "Branch-Guide  $-16$  dB LO directional couplers", IRAM Technical Report N. 263.02, Jan. 2002